A Structural Investigation of CaAOT/Water/Oil Microemulsions

ARTICLE *in* LANGMUIR · NOVEMBER 1999

Impact Factor: 4.46 · DOI: 10.1021/la990656+

4 AUTHORS, INCLUDING:

Ruggero Angelico
Università degli Studi del Molise
51 PUBLICATIONS **605** CITATIONS
SEE PROFILE

Olle Söderman
Lund University
210 PUBLICATIONS **6,314** CITATIONS
SEE PROFILE

Maura Monduzzi
Università degli studi di Cagliari
160 PUBLICATIONS **2,972** CITATIONS
SEE PROFILE

A Structural Investigation of CaAOT/Water/Oil Microemulsions

Paolo Pitzalis,[†] Ruggero Angelico,[‡] Olle Soderman,[§] and Maura Monduzzi*[,†]

Dipartimento Scienze Chimiche, Università di Cagliari, S.S. 554 Bivio Sestu, 09042 Monserrato, Italy, D.I.S.T.A.A.M., Università del Molise, Via De Sanctis, 86100 Campobasso, Italy, and Physical Chemistry 1, Centre for Chemistry and Chemical Engineering, Lund University, P.O. Box 124, S-221 00 Lund, Sweden

Received May 27, 1999. In Final Form: September 15, 1999

The microstructural features of ternary microemulsions in the CaAOT/water/isooctane system are investigated by conductivity and NMR self-diffusion measurements. The results are compared with the corresponding NaAOT system. Experimental data are collected along water and oil dilution lines with the aim of investigating the interactions among the surfactant aggregates. Previous studies on the microemulsion regions of CaAOT/water/decane are also considered in order to evaluate the influence of the oil (branched or linear) on the microstructural transitions. Water-in-oil spherical droplets with a hard-sphere behavior are likely to occur in a very limited region of the L_2 phase, namely, at low volume fractions of the disperse phase, ϕ_d. Both conductivity and water self-diffusion demonstrate the occurrence of important modifications of the water-in-oil droplet organization and suggest the occurrence of transient fusion−fission processes among the droplets. These processes become more and more important with increasing ϕ_d. The microstructure of the system is discussed in view of different approaches based on percolation theory, attractive interactions among discrete particles, and a multiconnected water network.

Introduction

The sodium salt of the di-chained anionic surfactant bis-2-ethylhexylsulfosuccinate (aerosol OT or simply NaAOT) forms water-in-oil (w/o) microemulsions without a cosurfactant in a wide range of temperatures and compositions. Many studies and review articles and several recent papers[1−13] have provided significant advances in the understanding of phase and microstructural transitions through different techniques. Most studies have considered mainly dilute regions of the L_2 phase. At a volume fraction of the dispersed phase $\phi_d = \phi_w + \phi_s < 0.1$ (subscripts w and s refer to water and surfactant, respectively), that is, close to the oil corner, the microstructure of AOT w/o microemulsions is reasonably well described in terms of spherical droplets.[14] So far, with increasing ϕ_d, discrepancies with respect to the hard-sphere model have been discussed in terms of strong interparticle interactions, microstructural transitions, and percolation behavior. These phenomena are oil- and temperature-dependent.[7,10,12,15] The short-range attractive interactions can produce clusters of droplets which, in turn, generate water networks throughout the L_2 phase. Important changes of the transport properties, such as diffusion and electrical conductivity, occur. The phenomena have been described in terms of "percolation".[10,13,16] Within the percolation theory, the conductivity along an oil dilution line can be reproduced by two separate asymptotic scaling power laws having different exponents below and above the percolation threshold:[16]

$$\sigma \approx (\phi_d^c - \phi_d)^{-s} \quad \text{at} \quad \phi_d < \phi_d^c$$

(below percolation threshold)

$$\sigma \approx (\phi_d - \phi_d^c)^t \quad \text{at} \quad \phi_d > \phi_d^c$$

(above percolation threshold)

Percolation occurs when the volume fraction of the dispersed phase ϕ_d reaches a critical value ϕ_d^c at constant temperature, when the temperature reaches a value T_c at constant ϕ_d, or when the water-to-surfactant (w/s) molar ratio increases. The critical exponent t generally ranges between 1.5 and 2, whereas the exponent s allows assignment of the time-dependent percolation regime. Thus, $s < 1$ (generally around 0.6) identifies a "static percolation" regime, and $s > 1$ (generally around 1.3) identifies a "dynamic percolation" regime. The static percolation is related to the appearance of bicontinuous microemulsions,[17] where the sharp increase of the conductivity, due to both counterions and, to a lesser extent, surfactant ions,[13] can be justified by a connected water

* To whom correspondence should be addressed. Tel.: 39-070-675 4385. Fax: 39-070-675 4388. E-mail: monduzzi@vaxca1.unica.it.
[†] Università di Cagliari.
[‡] Università del Molise.
[§] Lund University.

(1) Luisi, P. L.; Magid, L. *Crit. Rev. Biochem*. **1986**, *20*, 409.
(2) Carlstrom, G.; Halle, B. *Langmuir* **1988**, *6*, 1346−1352.
(3) Carlstrom, G.; Halle, B. *J. Phys. Chem*. **1989**, *93*, 3287−3299.
(4) Furó, I.; Halle, B.; Quist, P.; Wang, T. C. *J. Phys. Chem*. **1990**, *94*, 2600−2613.
(5) Halle, B. *Prog. Colloid Polym. Sci*. **1990**, *82*, 211.
(6) Eastoe, J.; Robinson, B. H.; Steytler, D. C.; Thorn-Leeson, D. *J. Colloid Interface Sci*. **1991**, *36*, 1−31.
(7) Kotlarchyk, M.; Sheu, E. Y.; Capel, M. *Phys. Rev. A* **1992**, *46*, 928.
(8) Kurumada, K.; Shioi, A.; Harada, M. *J. Phys. Chem*. **1994**, *98*, 12382.
(9) Kurumada, K.; Shioi, A.; Harada, M. *J. Phys. Chem*. **1995**, *99*, 16982.
(10) Feldman, Y.; Kozlovich, N.; Nir, I.; Garti, N. *Phys. Rev. E* **1995**, *51*, 478 and references therein.
(11) Bardez, E.; Vy, N. C.; Zemb, T. *Langmuir* **1995**, *11*, 3374.
(12) Berghenholtz, J.; Romagnoli, A.; Wagner, N. *Langmuir* **1995**, *11*, 1559.
(13) Feldman, Y.; Kozlovich, N.; Nir, I.; Garti, N.; Archpov, V.; Idiyatullin, Z.; Zuev, Y.; Fedotov, V. *J. Phys. Chem*. **1996**, *100*, 3745.
(14) Jahn, W.; Strey, R. *J. Phys. Chem*. **1988**, *92*, 2294.
(15) Cametti, C.; Codastefano, P.; Tartaglia, P.; Chen, S. H.; Rouch, J. *Phys. Rev. A* **1992**, *45*, 5359 and references therein.
(16) Ponton, A.; Bose, T. K.; Delbos, G. *J. Chem. Phys*. **1991**, *94*, 6879.
(17) deGennes, P. G. *J. Phys*. (*Paris*) **1980**, *41*, C13.

10.1021/la990656+ CCC: $19.00
Published on Web 11/16/1999

path in the system. The dynamic percolation[18] is related to rapid processes of fusion−fission among the droplets. Transient water channels form when the surfactant interface breakes down during collisions or through the merging of droplets. In this latter case, conductivity is mainly due to the motion of counterions along the water channels.[13]

The interpretation of these interactions in terms of static or dynamic percolation is obviously strictly dependent on the time-scale of the experimental technique.

The transition from bicontinuous to w/o droplets has been successfully described in terms of the geometrical disordered open connected (DOC) model.[19,20] The DOC model consists of spheres that are connected to Z nearest neighbors through cylinders. The number of connections for each sphere can be adjusted in order to mimic the dimension of the water domain. The DOC model has been shown to correctly predict conductivity and water self-diffusion data, along water dilution lines, in w/o microemulsions formed by the double-chained didodecyldimethylammonium bromide (DDAB) surfactant with several oils and also in the case of perfluoropolyether (PFPE) w/o microemulsions.[21,22] In those cases, a gradual transition of the microstructure from bicontinuity (Z_{max} = 13.4) to disconnected w/o droplets (Z_{min} = 0) with increasing water content has been suggested.

The interaggregate interactions are determined by the interplay of van der Waals and electrostatic forces, which determine the local curvature of the surfactant interface. The charge of the counterion is expected to play a crucial role on the electrostatic interactions and the hydration strength. In the case of the CaAOT/water binary system,[23,24] a significant reduction of the extension of the lamellar (L_α) region with respect to the corresponding sodium AOT/water system has been observed. Minor differences in the formation and range of existence of the bicontinuous cubic V_2 and of the reverse hexagonal H_2 phases are observed. Similarly, in the ternary system CaAOT/W/C10, the w/o microemulsion region shrinks significantly.[25] Experiments carried out within the whole microemulsion phase revealed a variety of interactions upon moving either on a water or an oil dilution line. Close to the oil corner, the interactions can be described in terms of charge fluctuations among small w/o droplets. With increasing surfactant and water content, the lifetime of the contacts among the droplets increases up to the identification of a structural transition from closed water domains to a connected water network through a gradual variation of the interconnectivity.

Few studies report on the w/o microemulsions formed by AOT with divalent counterions. It has been shown that w/o microemulsions formed by AOT with divalent counterions in cyclohexane oil consist of w/o spherical droplets at low w/s and ellipsoidal or cylindric particles at high w/s. Only for the CaAOT system has a structural behavior similar to NaAOT been suggested.[11,26−29] In the case of Co-, Cu-, and CdAOT/W/isooctane microemulsions, transitions from spherical droplets to interconnected cylinders have been suggested upon increasing the w/s ratio.[30] It should be noticed that for these bimetallic-AOT microemulsion systems, only limited ranges of the L_2 microemulsion region were examined, and the phase diagrams have never been reported.

In this work, the phase behavior of the microemulsion region of the ternary system CaAOT/water/isooctane (CaAOT/W/ISO) is investigated and compared with the NaAOT/W/ISO system, with specific emphasis on the effect of replacing the divalent Ca^{2+} for the monovalent Na^+ counterion. In addition, the comparison with data previously obtained for CaAOT/W/C10 microemulsions allows us to draw some conclusions on the influence of the oil shape and penetration.

Experimental Section

Materials. Bis-(2-ethylhexyl) sodium sulfosuccinate (AOT) and *n*-decane (C10) were purchased from Sigma-Aldrich, and trimethylpentane (isooctane) and calcium nitrate are Carlo Erba products. The calcium salt of AOT was prepared by aqueous metathesis of a saturated solution of $Ca(NO_3)_2$ with a methanolic solution of NaAOT. The CaAOT precipitate was recrystallized from methanol and then freeze-dried after solvent evaporation. The aqueous phase was separated by centrifugation and was washed repeatedly with distilled water to the complete disappearance of NO_3^- and Na^+ ions, as determined by the diphenylamine test (the solution becomes blue in the presence of nitrate ions) and by NMR.

Distilled water, with a conductivity <5 μS/cm at 25 °C, was used to prepare the samples.

Conductivity. The conductivity measurements were performed with an Orion 120 conductimeter, in the range 81 Hz − 41 MHz (the signal intensity depends on the sample conductivity). The electrodes were made from platinum, and the cell temperature was controlled to within ±0.5 ° C by a thermostatic bath.

To investigate water dilution lines, samples containing the surfactant−oil mixtures were transferred into a sealed thermostatted cell under stirring. The proper amount of freshly distilled water (kept in the thermostatic bath) was gradually added through a micropipet (estimated error 0.001 mL). After each water addition, the system was left under stirring for 20 min to achieve equilibrium. Conductivity measurements were done 1 min after stirring ceased.

To investigate the oil dilution lines, a batch sample at the proper w/s ratio and containing the minimum amount of oil to obtain an isotropic liquid phase was prepared. Then, the various samples along the oil dilution line were individually prepared by adding a weighed amount of oil to a weighed amount of the batch sample. Each sample was left to reach thermal equilibrium for 30 min before conductivity was measured.

NMR. ^{1}H NMR experiments were performed at 1.88 T on a Varian FT 80A spectrometer at the operating frequency of 80 MHz and at 4.7 T on a Bruker DMX 200 spectrometer at the operating frequency of 200 MHz. The temperature was always kept constant with a precision of ±0.5 °C.

Samples for NMR experiments were prepared by weighing the proper amount of the components directly in the NMR sample tube. The samples were homogenized by gentle mixing, then frozen for 12 h. The tubes were flame-sealed and stored at 25 °C for at least 1 week before any measurement was performed.

Diffusion measurements were performed using the Fourier transform pulsed gradient spin−echo (FT-PGSE) technique, as

(18) Grest, G.; Webman, I.; Safran, S.; Bug, A. *Phys. Rev. A* **1986**, *33*, 2842.
(19) Hyde, S. T. *J. Phys. Chem*. **1989**, *93*, 1458.
(20) Hyde, S. T.; Ninham, B. W.; Zemb, T. *J. Phys. Chem*. **1989**, *93*, 1464.
(21) Knackstedt, M. A.; Ninham, B. W. *Phys. Rev. E* **1994**, *50*, 2839 and reference therein.
(22) Monduzzi, M.; Knackstedt, M. A.; Ninham, B. W. *J. Phys. Chem*. **1995**, *99*, 17772.
(23) Khan, A.; Fontell, K.; Lindman, B. *J. Colloid Interface Sci*. **1984**, *101*, 193.
(24) Khan, A.; Jönsson, B.; Wennerström, H. *J. Phys. Chem*. **1985**, *89*, 5180.
(25) Caboi, F.; Capuzzi, G.; Baglioni, P.; Monduzzi, M. *J. Phys. Chem. B* **1997**, *101*, 10205.
(26) Bardez, E.; Larrey, B.; Zhu, X. X.; Valeur, B. *Chem. Phys. Lett*. **1990**, *171*, 362.
(27) Eastoe, J.; Fragneto, G.; Robinson, B. H.; Towey, T. F.; Heenan, R. K.; Leng, F. J. *J. Chem. Soc., Faraday Trans*. **1992**, *88*, 461−471.
(28) Eastoe, J.; Towey, T. F.; Robinson, B. H.; Williams, J.; Heenan, R. K. *J. Phys. Chem*. **1993**, *97*, 1459.
(29) Giordano, R.; Migliardo, P.; Wanderlingh, U.; Bardez, E. *J. Mol. Struct*. **1993**, *296*, 265.
(30) Petit, C.; Lixon, P.; Pileni, M. P. *Langmuir* **1991**, *7*, 2620.

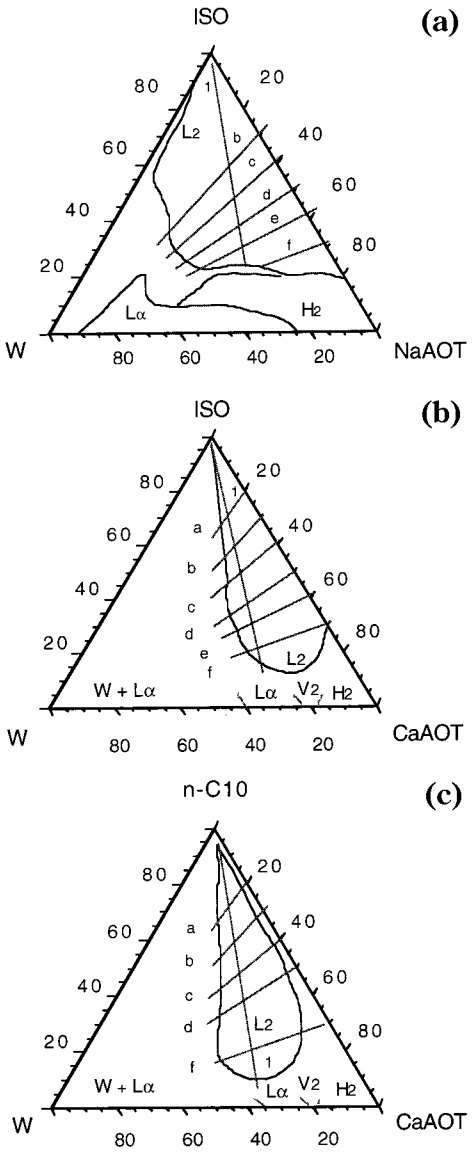

Figure 1. Partial phase diagrams at 25 °C. Line "1" indicates the oil dilution line at water/surfactant mass ratio ≈ 35/65 (molar ratio w/s ≈ 13). Lines "a"−"f" indicate the water dilution lines at the following s/o mass ratios: "a" = 2/8, "b" = 3/7, "c" = 4/6, "d" = 5/5, "e" = 6/4, and "f" = 7/3. (a) NaAOT/W/ISO redrawn from ref 33; (b) CaAOT/W/ISO; (c) CaAOT/W/DEC redrawn from ref 25.

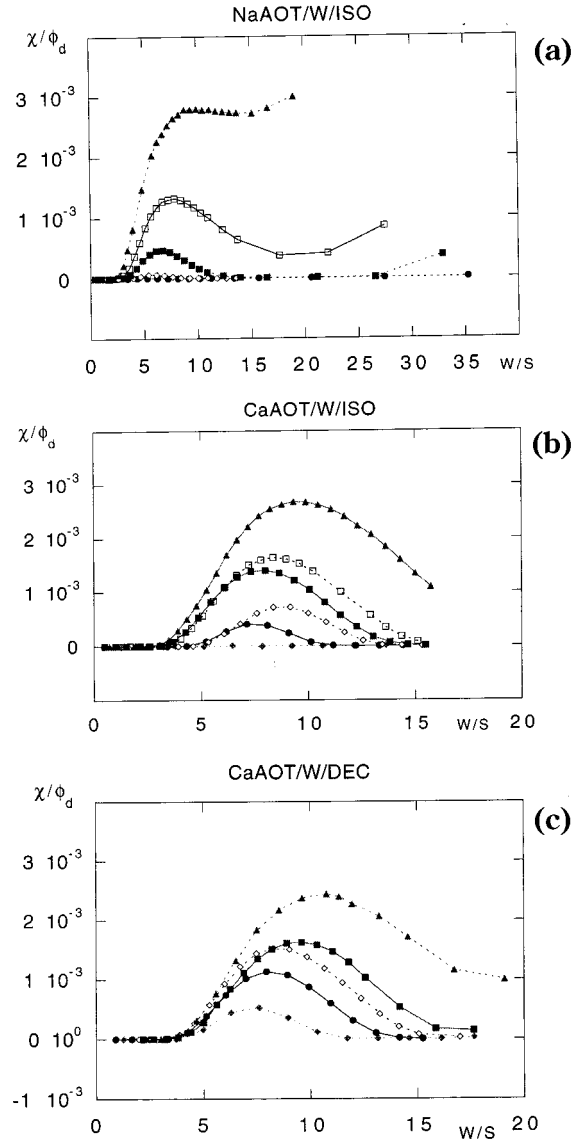

Figure 2. Normalized values of conductivity (χ/ϕ_d) at 25 °C along the water dilution lines as a function of the molar ratio w/s = [H_2O]/[AOT^-]: (a) NaAOT/W/ISO, [●] line "b", [◇] line "c", [■] line "d", [□] line "e", [▲] line "f"; (b) CaAOT/W/ISO, [◆] line "a", [●] line "b", [◇] line "c", [■] line "d", [□] line "e", [▲] line "f"; (c) CaAOT/W/DEC, [◆] line "a", [●] line "b", [◇] line "c", [■] line "d", [▲] line "f".

described by Stilbs.[31,32] The experiments were carried out by varying the gradient pulse length (δ) while keeping the gradient strength (G) and the pulse interval (Δ) constant. The decay of the echo intensity with increasing values of δ is given by

$$A(\delta) = A_0 \exp[-D(\gamma G\delta)^2(\Delta - \delta/3)] \quad (1)$$

where D is the self-diffusion coefficient, A_0 is the echo intensity in the absence of any gradient, and γ the magnetogyric ratio. Due to short spin−spin relaxation times of the NMR signals, surfactant self-diffusion coefficients have been determined through the stimulated echo pulse sequence[32] performed on the DMX 200 spectrometer, by varying G and keeping δ and Δ constant, to improve the signal-to-noise ratio.

The self-diffusion coefficients were calculated by means of a two-parameter nonlinear fit of eq 1. The error in the measurements, as judged by repeated measurements, is estimated to be smaller than ±5%.

Results and Discussion

1. Phase Diagrams. The phase diagrams of the ternary systems are reported in Figure 1. In Figure 1a, the phase diagram of NaAOT/W/ISO is redrawn from literature data.[33] Figure 1b and 1c shows the CaAOT/W/ISO and CaAOT/W/DEC [25] phase diagrams. The L_2 phase boundaries have been determined with an accuracy of ±1 wt %. The amount of the oil uptake of the various liquid crystalline phases of the CaAOT/W binary system has not been accurately determined. The "a"−"f" water dilution lines which, with the oil dilution line (line 1 in the phase diagrams of Figure 1), have been investigated are also shown. The oil dilution line was chosen at a water/surfactant = 35/65 mass ratio in all systems, which

(31) Stejskal, E. O.; Tanner, J. E. *J. Chem. Phys.* **1965**, *42*, 288.
(32) Stilbs, P. *Prog. Nucl. Magn. Reson. Specrosc.* **1987**, *19*, 1 and reference therein.
(33) Tamamushi, B.; Watanabe, N. *Colloid Polym. Sci.* **1980**, *258*, 174.

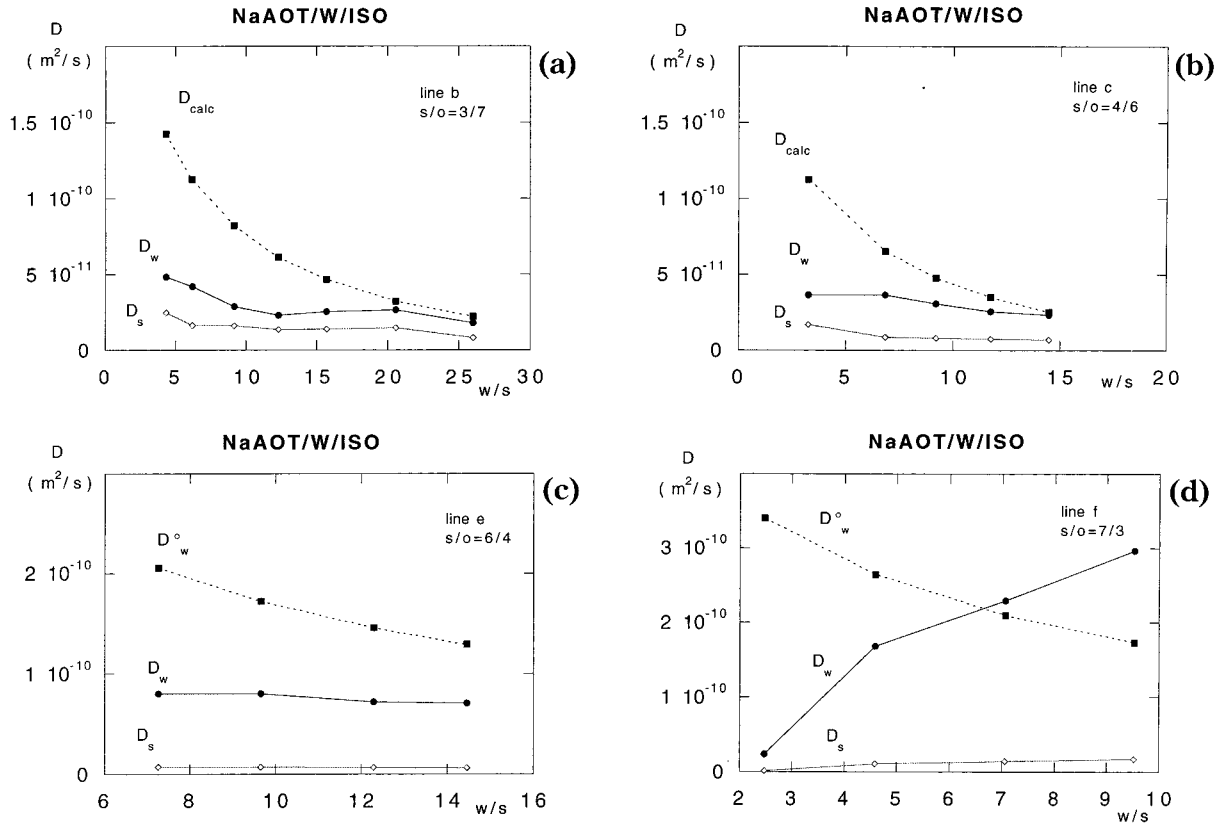

Figure 3. Water D_w [●] and surfactant D_s [◇] self-diffusion coefficients, together with D_{calc} (eq 4) or $D_w°$ (eq 3) [■] vs w/s at 25 °C, along the water dilution lines of the NaAOT/W/ISO system: (a) line "b"; (b) line "c"; (c) line "e"; (d) line "f".

approximately corresponds to 13.2 water molecules per polar head (w/s).

As already discussed in previous papers,[25,34] the significant shrinkage of the microemulsion region upon replacing Na^+ with a Ca^{2+} counterion can be related to a decrease of the electrostatic repulsion among surfactant headgroups induced by a higher Ca^{2+} binding at the interface. The expected increase of the effective hydrophobic volume of 2 [AOT^-] entities, strictly interconnected for electrostatic reasons, seems to account well for a limited water uptake. The negative interfacial curvature is not allowed to approach zero values in the presence of a penetrating oil. In related studies, Khan et al.[23,24] suggested that the L_α phase of the CaAOT/W binary system cannot be swollen by water to the same extent as for the case of NaAOT for electrostatic reasons. Differently from NaAOT, the CaAOT surfactant has been shown to be insoluble in *n*-decane,[25] and the formation of the microemulsion requires the addition of at least 2 wt % of water and extends to a maximum water uptake of about 40 wt %. However, with isoctane, CaAOT is again oil-soluble, while the microemulsion region shows a maximum water uptake of about 30 wt %. These data should be compared with a water uptake of around 50 wt % reported for the microemulsion in NaAOT/W/ISO.

2. Water Dilution Lines. The water dilution lines, referred to as "a"−"f" lines in the phase diagrams of Figure 1, were investigated through conductivity and NMR self-diffusion.

Figure 2 shows the conductivity curves measured as a function of the molar ratio w/s = $[H_2O]/[AOT^-]$, normalized[5] with respect to the volume fraction of the dispersed phase $\phi_d = \phi_s + \phi_w$, where ϕ_s and ϕ_w are the volume fractions of surfactant and water, respectively. The data for the CaAOT/W/DEC system are redrawn from ref 25. The data for line "a" of the NaAOT/W/ISO system are not reported since negligible conductivities are measured at all w/s values.

Most of the conductivity curves appear as bell-shaped. Maxima increase with increasing s/o mass ratio. For lines "b" and "c" of the NaAOT/W/ISO system and line "a" of the CaAOT/W/ISO system, conductivity values at the maximum range between 1.5 and 20 μS/cm. These values can be justified in terms of charge fluctuations among the w/o droplets.[5] Line "b" of CaAOT/W/ISO and line "a" of CaAOT/W/DEC show maxima around 100 μS/cm, which exceed significantly the typical values found in the charge fluctuation model. However, the microstructure can still be considered as w/o droplets having interactions on the same time-scale as the observation time. The other conductivity lines display maxima which are well above the limits of a charge fluctuation model and should be considered as indicative of microstructural transitions of the polar domain. According to previous interpretations of similar trends,[21,35,36] conductivity data can be interpreted as percolative phenomena or in terms of the geometrical DOC model based on a variable interconnectivity of the water microdomains. With increasing w/s, the conductivity increases sharply 2−6 orders of magnitude (depending on s/o ratio) due to the progressive hydration of the polar groups. Maxima of conductivity occur at w/s ≈ 6−8. It seems plausible that the completion of the minimum hydration of the polar groups favors the formation of continuous water networks. Indeed, the question as to

(34) Capuzzi, G.; Pini, F.; Gambi, C. M. C.; Monduzzi, M.; Baglioni, P. *Langmuir* **1997**, *13*, 6927.

(35) Hyde, S.; Andersson, S.; Larsson, K.; Blum, Z.; Landh, T.; Lidin, S.; Ninham, B. W. *The Language of Shape*; Elsevier: Amsterdam, 1997.

(36) Caboi, F.; Monduzzi, M. *Prog. Colloid Polym. Sci.* **1998**, *108*, 153.

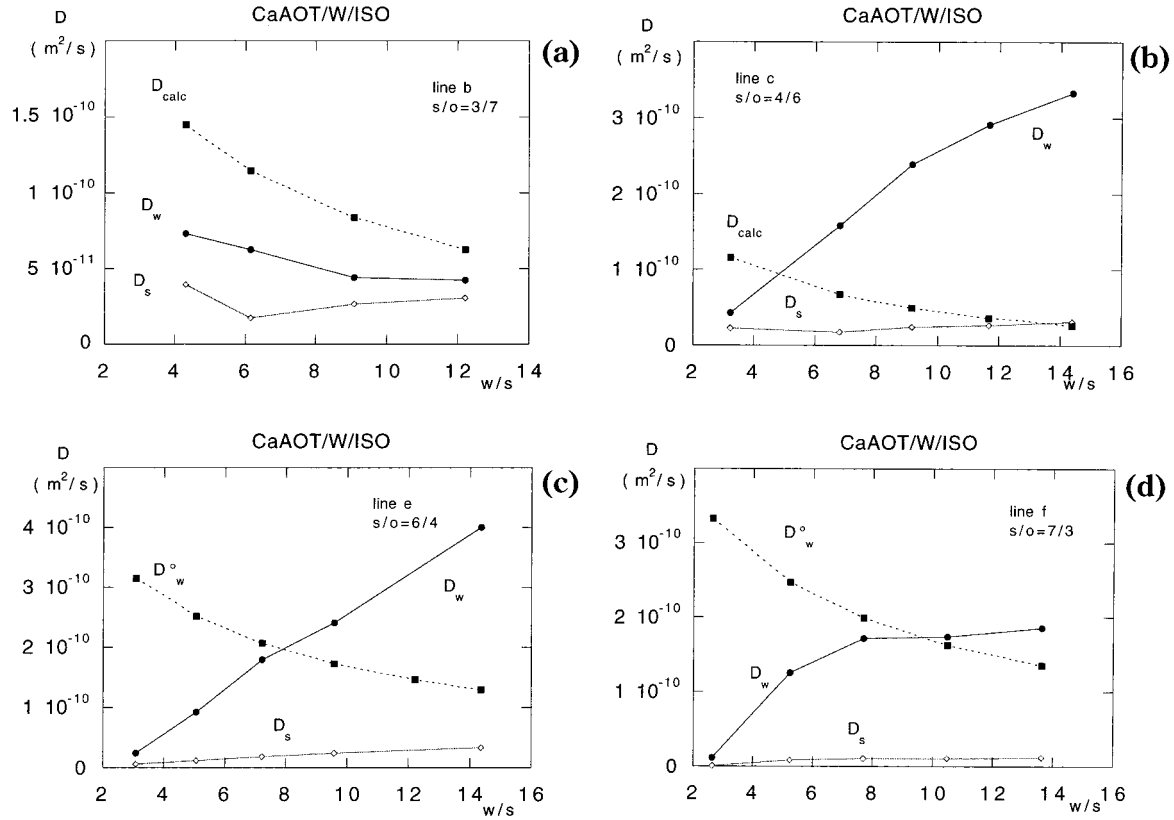

Figure 4. Water D_w [●] and surfactant D_s [◇] self-diffusion coefficients, together with D_{calc} (eq 4) or $D_w°$ (eq 3) [■] vs w/s at 25 °C, along the water dilution lines of the CaAOT/W/ISO system: (a) line "b"; (b) line "c"; (c) line "e"; (d) line "f".

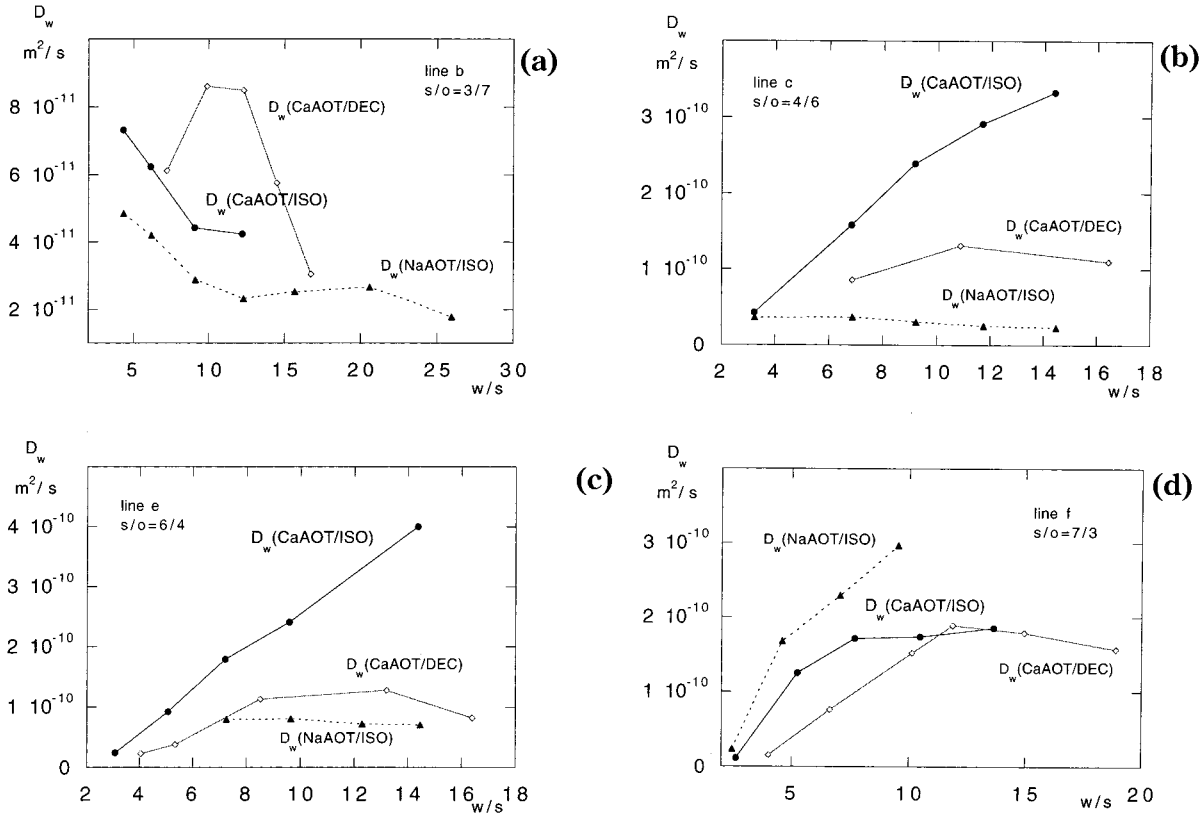

Figure 5. Water D_w self-diffusion coefficients for NaAOT/W/ISO [▲], CaAOT/W/ISO[●], and CaAOT/W/DEC[25] [◇] systems at the various s/o ratios: (a) line "b"; (b) line "c"; (c) line "e"; (d) line "f".

what type of microstructure exists at w/s < 6 remains unanswered. Further addition of water, beyond w/s ≈ 6−8, causes a decrease of conductivity. The water domains evidently tend to disconnect to closed droplets, which at low s/o ratios should have a spherical shape (see below eq 3). At high surfactant concentrations, that is, for s/o ≥ 1, conductivity does not become negligible at high w/s in the vicinity of the phase boundary. Strongly interacting w/o

Table 1. Experimental $F(r) = D_w/D_w°$ Values and r_{prol}, r_{obl} Axial Ratios Calculated for Prolate and Oblate Shapes for NaAOT/W/ISO Lines "b" and "c", CaAOT/W/ISO Line "b", and CaAOT/W/DEC Line "a"

NaAOT/W/ISO line b				NaAOT/W/ISO line c			
w/s	$D_w/D_w°$	r_{prol}	r_{obl}	w/s	$D_w/D_w°$	r_{prol}	r_{obl}
4.41	0.34	8.4	4.0	3.25	0.33	8.9	4.2
6.32	0.37	7.3	3.6	6.82	0.60	3.3	2.0
9.26	0.30	10.5	4.8	9.21	0.64	2.8	1.8
12.49	0.40	6.5	3.3	11.91	0.78	1.9	1.4
16.02	0.48	4.8	2.7	14.51	0.97	1.1	1.0
20.87	0.73	2.1	1.6				
26.46	0.85	1.5	1.3				

CaAOT/W/ISO line b				CaAOT/W/DEC line a			
w/s	$D_w/D_w°$	r_{prol}	r_{obl}	w/s	$D_w/D_w°$	r_{prol}	r_{obl}
4.38	0.34	8.4	4.1	7.01	0.79	1.8	1.4
6.28	0.47	4.9	2.7	9.04	0.94	1.2	1.1
9.20	0.40	6.3	3.3	15.02	1.03	-	-
12.41	0.48	4.7	2.6	17.24	0.67	2.6	1.7

droplets or a partially connected water domain are possible explanations for this behavior. Obviously, this picture should be referred to the experimental time-scale. Finally, for line "f", at s/o = 7/3, no maxima can be clearly identified in any of the three systems. Indeed, the systems phase-separate without reaching the curvature constraints required for closed interfaces.

The conductivity data are qualitatively paralleled by the water and surfactant self-diffusion coefficients. The experimental D_w and D_s values, obtained for the various s/o ratios of the NaAOT/W/ISO and CaAOT/W/ISO systems, are reported in Figure 3 and Figure 4, respectively.

Before discussing the diffusion results, it should be recalled that the self-diffusion coefficient of pure water at 25 °C is 2.29×10^{-9} m²/s.[37] Assuming that a spherical droplet model holds along the water dilution lines, the droplet radius R_d is expected to increase with increasing w/s according to the geometrical constraints

$$R_d\,(\text{nm}) = (3V_w/\sigma)(\text{w/s}) + l = 0.175\,(\text{w/s}) + 0.85 \qquad (2)$$

where $V_w = 0.035$ nm³ is the volume of a water molecule, $\sigma = 0.6$ nm² is the area of the polar head, and $l = 0.85$ nm is the average length of the surfactant chain. Consequently, the D_w values are expected to decrease following the usual Stokes−Einstein relation:

$$D_w° = kT/6\pi\eta\, R_d \qquad (3)$$

where η is the viscosity of the medium. Equation 3 is rigorously valid at infinite dilution. In fact, $D_w°$ usually decreases with an increase in volume of the dispersed phase ϕ_d. Thus, at finite concentration

$$D_{calc} = D_w°\,(1 - \alpha\,\phi_d) \qquad (4)$$

where $\alpha = 2$ is the typical obstruction factor in the absence of hydrodynamic interactions.[38,39] Obviously, eq 4 is valid for $\phi_d < 0.5$. Figure 3 and Figure 4 show the D_{calc} (for $\phi_d < 0.5$) or, alternatively, the $D_w°$ values (for $\phi_d > 0.5$) together with the experimental diffusion coefficients.

The experimental results show the following peculiarities:

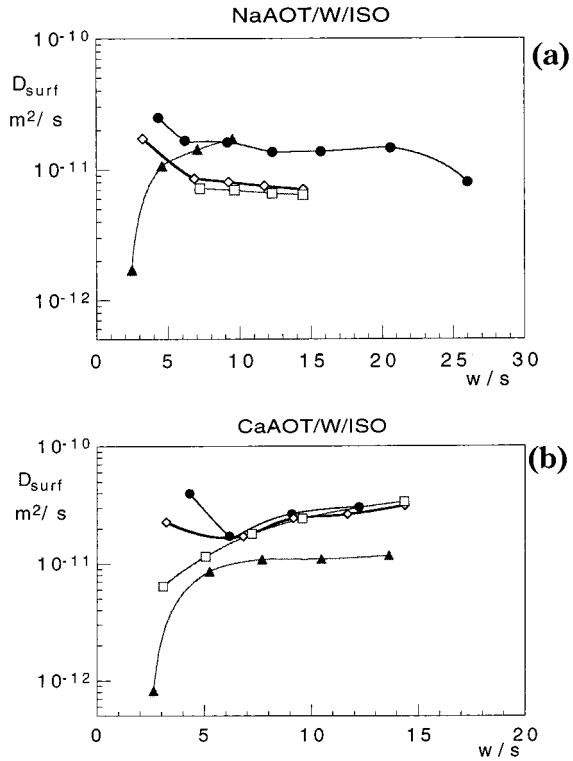

Figure 6. Surfactant self-diffusion coefficients D_{surf} vs w/s at 25 °C, along the water dilution lines: (a) NaAOT/W/ISO, [●] line "b", [◇] line "c", [□] line "e", [▲] line "f"; (b) CaAOT/W/ISO, [●] line "b", [◇] line "c", [□] line "e", [▲] line "f".

(i) The system NaAOT/W/ISO (cf. Figure 3) shows D_w coefficients which decrease with increasing w/s for "b", "c", and "e" dilution lines with values in the range $(2-8) \times 10^{-11}$ m²/s. These values are indicative of closed water domains. A different trend and a substantial increase of the D_w values above 10^{-10} m²/s is found for line "f". The existence of w/o droplets, almost monodisperse in size and shape, can be suggested along lines "b" and "c", since similar values for D_w and D_s self-diffusion coefficients are observed. For line "e", D_s is 1 order of magnitude smaller than D_w, while the difference between the two values increases significantly for line "f".

(ii) For the CaAOT/W/ISO system (cf. Figure 4), only lines "b" and "c" show a decreasing trend with increasing w/s, with D_w coefficients in the range $3-12 \times 10^{-11}$ m²/s. The other dilution lines show an increase of D_w with increasing w/s. Rather similar values of D_w and D_s self-diffusion coefficients are observed along line "b" and at very low water content along lines "c", "e", and "f".

Provided that D_w values higher than 10^{-10} m²/s generally indicate the occurrence of a continuous water domain,[40] it is not easy, however, to discriminate between closed and connected water domains. The comparison between the experimental D_w values and those calculated by eq 4 makes it evident that spherical droplets are seldom present except along lines "b" and "c" of NaAOT/W/ISO at high w/s. Similarly, the experimental D_w values measured for line "a" of the CaAOT/W/DEC system at w/s > 8, previously investigated,[25] were rather well reproduced by eq 4.

In several cases, at low s/o ratios, the experimental D_w decreases more than expected for spherical droplets. This may suggest the occurrence of closed nonspherical water domains such as prolate or oblate shapes.

(37) Mills, R. *J. Phys. Chem.* **1973**, *77*, 685.
(38) Ohtsuki, T.; Okano, K. *J. Chem. Phys.* **1982**, *77*, 1443.
(39) Lekkerkerker, H. N. W.; Dhont, J. K. G. *J. Chem. Phys.* **1984**, *80*, 5790.
(40) Guering, P.; Lindman, B. *Langmuir* **1985**, *1*, 464.

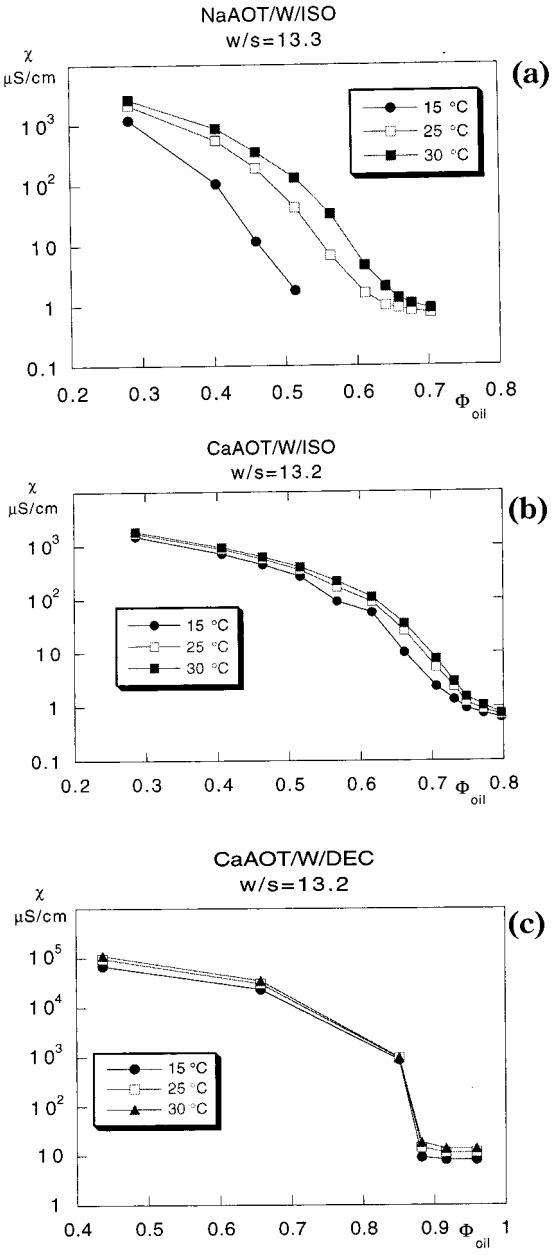

Figure 7. Conductivity along oil dilution line "1" as a function of the oil volume fraction Φ_{oil} at [●] 15 °C, [□] 25 °C, and [▲] 30 °C: (a) NaAOT/W/ISO; (b) CaAOT/W/ISO; (c) CaAOT/W/DEC redrawn from ref 25.

According to previous papers,[41] the D_w of a w/o droplet decreases as the axial ratio $r = a/b$ (where $b = R_d$ is the minor axis) of the prolate and oblate shape increases. Thus

$$D_{prol/obl} = D_w^{\circ} F(r)$$

where $F(r)$ is

$$F(r) = \{\ln[r + (r^2 - 1)^{0.5}]\}/(r^2 - 1)^{0.5}$$

for prolate shape and

$$F(r) = \{\arctan[(r^2 - 1)^{0.5}]\}/(r^2 - 1)^{0.5}$$

for oblate shape. Table 1 reports the $F(r) = D_w/D_w^{\circ}$ and the corresponding r axial ratio calculated for the cases of

(41) Balinov, B.; Olsson, U.; Soderman, O. *J. Phys. Chem.* **1991**, *95*, 5931.

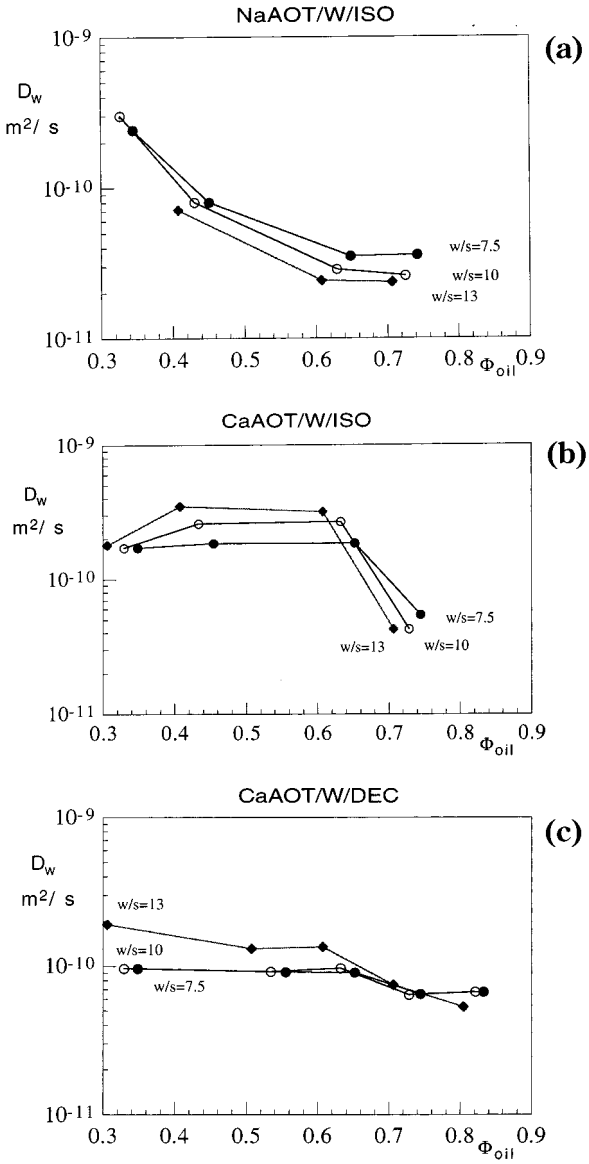

Figure 8. Water self-diffusion coefficients D_w vs Φ_{oil} at 25 °C, along the oil dilution lines at the molar ratios: [●] w/s = 7.5, [○] w/s = 10, and [◆] w/s = 13: (a) NaAOT/W/ISO; (b) CaAOT/W/ISO; (c) CaAOT/W/DEC redrawn from ref 25.

lines "b" and "c" of the NaAOT/W/ISO system, line "b" of the CaAOT/W/ISO system, and line "a" of the CaAOT/W/DEC system. Axial ratios are rather high at low w/s, whereas they tend to decrease as the phase boundary, at high w/s, is approached. It can be suggested that at low water content, important deviations from spherical shape occur as a consequence of various effects such as the incomplete hydration of the polar groups. This should favor the formation of cylindrical shapes, since the optimal interfacial curvature cannot be obtained. In addition, besides hydration effects, the balance between oil penetration and water volume fraction is crucial to determine the preferred curvature. Here, it is interesting to compare the D_w values obtained for the three systems, as reported in Figure 5, where the substantial differences observed between CaAOT systems upon replacing DEC with ISO, in comparison with NaAOT system, can be clearly seen.

For a comparison between NaAOT/W/ISO and CaAOT/W/ISO systems, it is convenient to also report together the surfactant self-diffusion coefficients, measured along "b", "c", "e", and "f" water dilution lines. Experimental D_{surf} values are reported in Figure 6. The largest variations

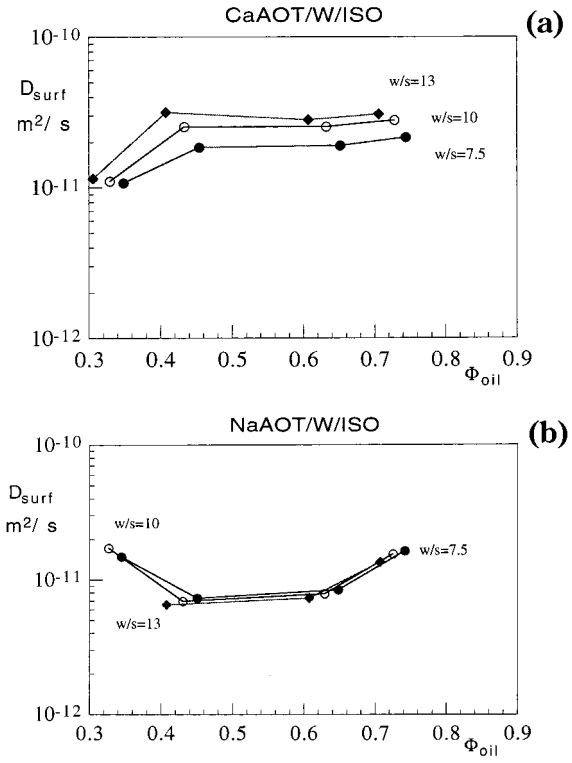

Figure 9. Surfactant self-diffusion coefficients D_{surf} vs Φ_{oil} at 25 °C, along the oil dilution lines at the molar ratios: [●] w/s = 7.5, [○] w/s = 10, and [◆] w/s = 13: (a) NaAOT/W/ISO; (b) CaAOT/W/ISO.

of D_{surf} values are found at low w/s. With increasing s/o ratios D_{surf} values decrease more than 1 order of magnitude on moving from line "b" to line "f" for both NaAOT and CaAOT systems. This can be easily related to the increase of surfactant concentration and then to the thickening of surfactant aggregates which, because of the low amount of water molecules per polar head (less than 5), cannot reach the typical mobility of small spherical w/o droplets, particularly in concentrated systems. At w/s > 6, the D_{surf} values of NaAOT level out at around 8×10^{-12} m^2/s for lines "c" and "e" and around 1×10^{-11} m^2/s for lines "b", and "f". For the CaAOT system, at w/s > 6, D_{surf} values in the range $(1-3) \times 10^{-11}$ m^2/s for lines "b", "c", and "e" are observed (values increase with increasing w/s), whereas for line "f", D_{surf} is around $(0.9-9) \times 10^{-11}$ m^2/s. The observed trends seem to indicate that the most significant structural variations occur around w/s = 5−6, that is, upon completing the minimum hydration required to promote the formation of regular aggregates. The surfactant diffusion is probably determined by lateral diffusion contributions along the curved surface, almost independently of the interconnectivity of the water domain.

3. Oil Dilution Lines. Conductivity measurements were performed at 15, 25, and 30 °C, along the oil dilution line at constant w/s ≈ 13 (reported as line "1" in the phase diagrams of Figure 1). Conductivity data are shown in Figure 7a and 7b for NaAOT and CaAOT/W/ISO systems, respectively. In Figure 7c, the data previously obtained for CaAOT/W/DEC are also reported for comparison. In the latter case, it was found that conductivity trends were almost independent of temperature in the examined range. A percolation threshold was clearly identified at the critical volume fraction of the dispersed phase around $\phi_d^c \approx 0.14$, being a rather well-defined inflection point. The interpretation of data in terms of percolation theory led to values of the critical exponents of $s = -0.64$ and $t = 1.58$,

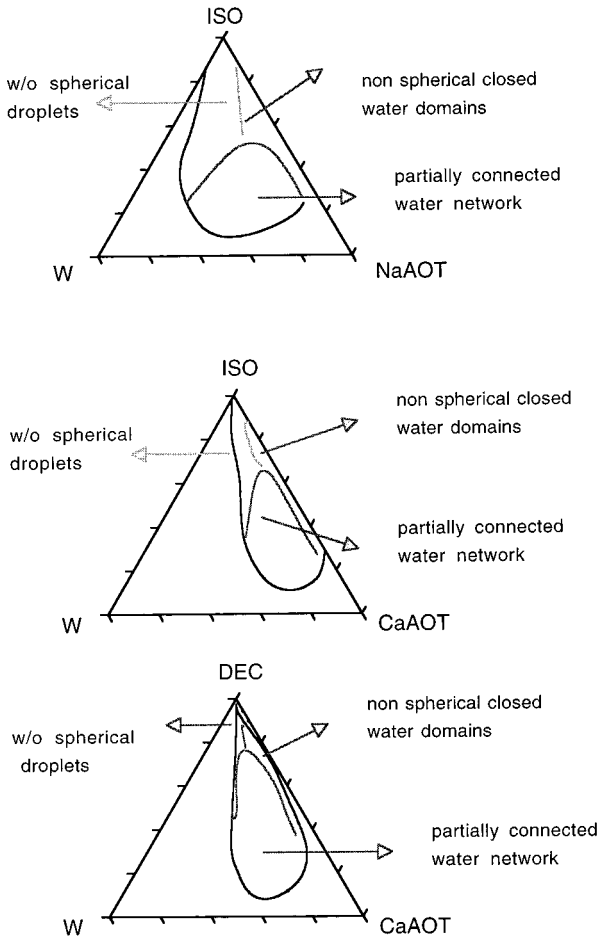

Figure 10. Schematic phase diagrams showing the regions of closed and partially connected water domains: (a) NaAOT/W/ISO; (b) CaAOT/W/ISO; (c) CaAOT/W/DEC.

which are typical of static percolation. The attempt to discriminate between static and dynamic percolation for the cases of NaAOT/W/ISO and CaAOT/W/ISO systems has failed, since ambiguous values of the critical exponents were calculated. This fact can be attributed to the evaluation of the percolation threshold in terms of volume fraction of the dispersed phase: this becomes crucial when inflection points cannot be clearly identified. From the temperature dependence of the conductivity curves, it can be deduced that in the case of the NaAOT system, dynamic percolation should occur at high volume fractions of the dispersed phase (low ϕ_{oil}). For the CaAOT/W/ISO system, although the critical volume cannot be clearly identified, static percolation is likely to occur at high volume fractions of the dispersed phase (low ϕ_{oil}), when the conductivity curves are almost coincident.

More significant indications are obtained by considering the trend of water and surfactant self-diffusion data along three different oil dilution lines, namely, w/s = 7.5, 10, and 13. D_w and D_{surf} values, at 25 °C, are reported in Figure 8 and Figure 9, respectively. For the CaAOT/W/DEC system, only D_w data are available, since they are taken from a previous work. The first observation is that both water and surfactant self-diffusion are almost independent of the w/s ratio, showing negligible differences among the curves of each system. For ISO systems, it can be remarked that at high oil volume fractions, similar values of D_w and D_{surf} are found for the two systems. This is what can be expected for the formation of w/o spherical droplets. Such a microstructure is, however, approached through different mechanisms, as is also indicated by the different

trends found for the surfactant diffusion. In the case of the NaAOT system, a gradual decrease of the size of the water domain accounts for the monotonic decrease of D_w. From the D_{surf} trends, it can be suggested that in the intermediate range, $\phi_{oil} = 0.45-0.65$, the decrease of surfactant diffusion is caused by the polydispersity of the aggregates (in terms of shape and size). In other words, the interactions among the aggregates can be considered to occur over a longer lifetime. At $\phi_{oil} > 0.75$, more regular and smaller aggregates form, thus determining lower lifetime interactions and an increase of D_{surf}. The $D_w \geq 10^{-10}$ and $D_{surf} \geq 10^{-11}$ m^2/s observed for the CaAOT system are likely to be due to the presence of interconnected clusters of aggregates. The comparison between the two CaAOT systems is a further indication of the strong effect due to the oil type and penetration, as already evidenced by conductivity data and percolation behavior as well as along the water dilution lines. In the case of CaAOT/W/DEC systems, in fact, the high values of D_w at $\phi_{oil} \approx 0.8$ indicate the occurrence of a significant degree of interaction at the level of the water domains.

Concluding Remarks

In this work, the effect of the counterion and of the oil shape on the microstructure of w/o microemulsions has been investigated through conductivity and NMR self-diffusion. At a macroscopic level, the replacement of the monovalent Na^+ with the divalent Ca^{2+} counterion causes a significant decrease of water uptake in the microemulsion region of the ternary phase diagrams.

The analysis of transport properties indicates that the occurrence of nonspherical shapes of the particles, the polydispersity, and the interdroplet attractive interactions induces a noticeable variety of microstructural features and transitions. It might be concluded that the current theories are unable to produce a suitable model to interpret the variety of the dynamic processes occurring, on the investigated time scale, upon changing the composition of the ternary systems. According to the present work, Figure 10 illustrates the microemulsion regions where spherical w/o droplets, nonspherical water-closed domains, and interconnected (at various degree) water networks are allowed to exist. Some other peculiar results deserve to be mentioned. NaAOT is almost freely soluble either in ISO or DEC oil, whereas CaAOT is soluble only in the ISO oil. CaAOT is likely to form reverse micelles in ISO, as reported for NaAOT in several oils. Therefore, the low conductivity values measured along line "a" of the CaAOT/W/ISO system is in agreement with the presence of w/o droplets in the regime of charge fluctuation. For the CaAOT/W/DEC system, line "a" shows a much higher conductivity maximum (2 orders of magnitude), which can be more likely related to the existence of a partially connected water network rather than to strong attractive interdroplet interactions. Indeed, due to the different shape, DEC oil does not allow the formation of any type of CaAOT aggregate without water.

Another interesting result is the significant variation of the surfactant self-diffusion coefficients, D_{surf}, at low water content (w/s < 6) with an increase in the s/o mass ratios, as shown in Figure 6. At w/s ≥ 7.5, as shown in Figure 9, D_{surf} values level out at around 10^{-11} m^2/s, independently of the composition. These observations support the suggestion that surfactant diffusion is mainly determined by lateral diffusion along the curved interface, provided that a sufficient hydration of the polar groups occurs.

Acknowledgment. MURST(Italy), CNR (Italy), Consorzio Sistemi Grande Interfase (CSGI-Firenze) and Assessorato Igiene Sanita' (Sardinia Region-Cagliari) are acknowledged for support. Bjorn Håkansson of the FK1 (Lund University, Sweden) is thanked for help during the acquisition of NMR data. Ali Khan (Lund University, Sweden) is also thanked for useful discussions.

LA990656+